A new aluminium electrolysis cell busbar network concept

Marc Dupuis
Consultant, GeniSim Inc., Québec, Canada
Corresponding author: marc.dupuis@genisim.com

Abstract

In recent years, the author has presented results of magnetohydrodynamic (MHD) cell stability studies obtained using a completely new busbar network concept. This new busbar concept has the advantage of being easily extendable to any cell size. To date, results have been presented for cells operating at 500 and 740 kA in an article published in the magazine ALUMINIUM in May 2006, for a cell operating at 600 kA in an article of the magazine ALUMINIUM in February 2011 and finally, for a cell operating at 1500 kA in an article of the magazine ALUMINIUM in February 2014. This paper presents in detail, for the first time, this new cell busbar network concept, and presents in more detail some of the MHD cell stability studies that were carried out to test its validity.

Keywords: MHD cell stability; busbar design; mathematical modeling.

1. Introduction

A considerable amount of literature is available on the subject of MHD cell stability. It turns out that the main factor influencing cell stability is the magnitude of the vertical component of the magnetic field (B_z) in the metal pad, or more precisely, the gradient between the positive value of the B_z at one end of the cell, and the negative value of the B_z at the other end. Urata [1] described the wave dynamics of a combined (2, 0) gravity mode wave with a (0, 1) gravity mode wave generating an MHD-driven rotating wave due to the presence of the longitudinal B_z gradient.

In Chapter 11 of his MHD book, Davidson [2] complements the Urata description by explaining how mechanical energy can be pumped into that system - energy that is required to grow an initial perturbation in order to generate and then sustain a high amplitude MHD wave. According to his work, the most probable MHD-driven rotating wave is a combined (3, 0) gravity mode with a (0, 1) gravity mode. This small discrepancy with Urata's work can be explained by the increase of the cell aspect ratio that was close to 2 to 1 when cell amperage was below 200 kA, and is now closer to 3 - 4 to 1 with cell amperage above 350 kA.

2. State of the art in busbar design

The magnetic field in the metal pad of a cell is generated by all the currents flowing in and around the cell. The major contributor of the magnetic field, and especially of its vertical component, B_z, is the network of busbars carrying the current from one cell to the next, as well as the return pot row. This is the reason why the proper design of the network of busbars and the location of the return pot row are so critical to cell stability.

Currently, three busbar network concepts are being used in the industry for high amperage cells. The first concept consists of designing an asymmetric busbar network that minimizes the B_z by mixing busbar paths, such as directing some busbars under the cell and some around the cell. The busbar network is typically not symmetric because it must compensate for the asymmetric effect of the return pot row in order to produce a symmetric magnetic field. This is the preferred approach for busbar network design for high amperage cells in China for example. A recent paper [3] presents and compares several Chinese busbar network designs for 400 kA cells. Figure 1 shows model-drawn 3-D perspective view of four Chinese busbar designs.

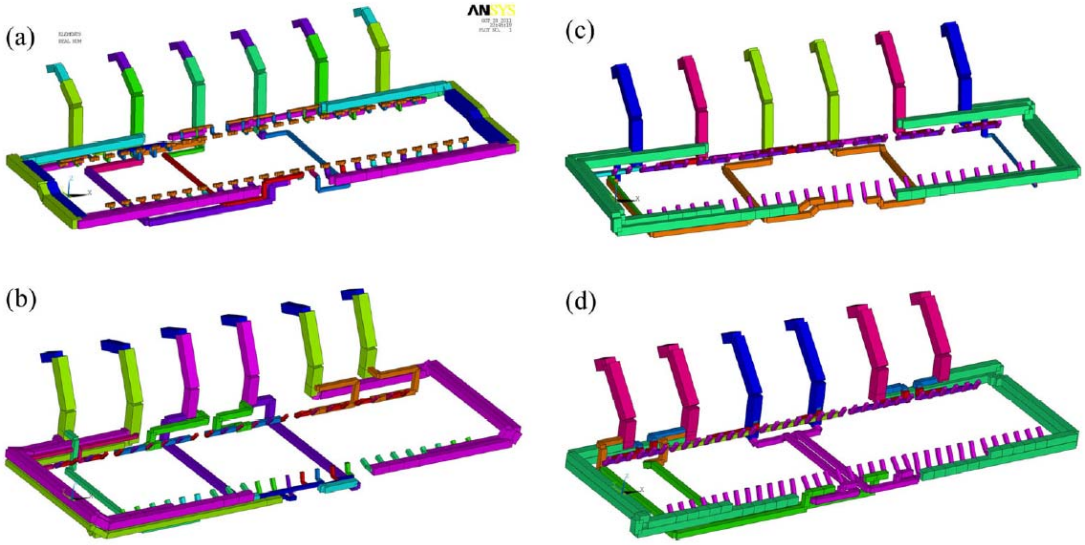

Figure 1. Busbar model of four 400 kA cells: (a) GY420; (b) SY400; (c) NEU400; (d) QY400 (Figure 4 of [3]).

As presented in Figure 5 and Table 4 of [3], all four designs produce fairly symmetric B_z magnetic fields within the range of ± 4.0 mT which according to [3], satisfies the *"basic magnetic field stability rules"*.

Figure 2 presents the model setup of a 500 kA cell using the first busbar concept as developed by the author, and presented in Figure 1 of [4]. Figure 3 shows the B_z field, generated by this design, also presented in Figure 1 of [4]. The B_z magnetic field is fairly symmetric within the range of ± 1.4 mT.

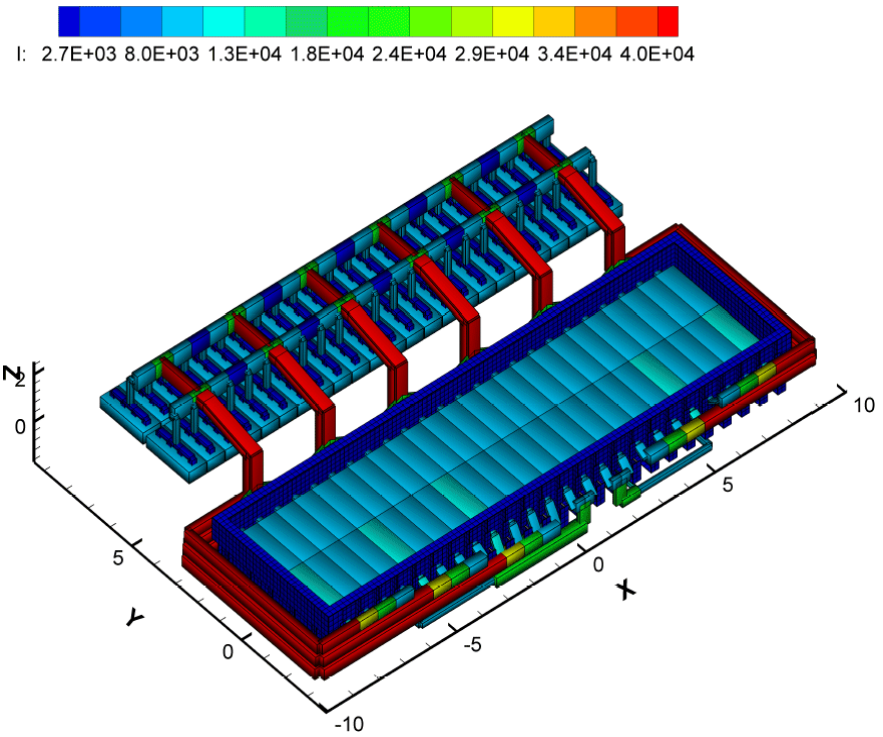

Figure 2. Busbar design of a 500 kA cell shown in Figure 1 of [4].

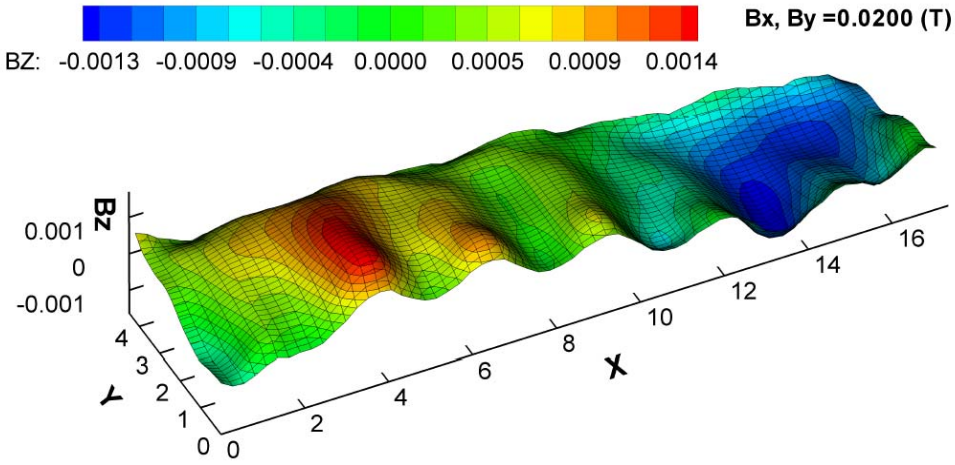

Figure 3. B_z of the busbar design in Figure 1, also shown in Figure 1 of [4].

The second busbar concept was patented by Pechiney in 1987 [5] and is assumed that it was meant to be the concept used for the AP60 busbar network of Rio Tinto's (RT's) 600 kA cell technology. In this busbar concept, 100 % of the current coming from the upstream side collector busbars passes under the cell, which is the shortest path possible. This generates a large B_z longitudinal gradient that must be neutralized by passing extra current in compensation busbars at the two ends of the cell. Figure 4 shows a possible application of this concept using eight risers and presumably 64 carbon anode blocks. (Risers are the busbars connecting cathode busbars of one cell to anode beam of next cell; they are also called anode risers or positive risers).

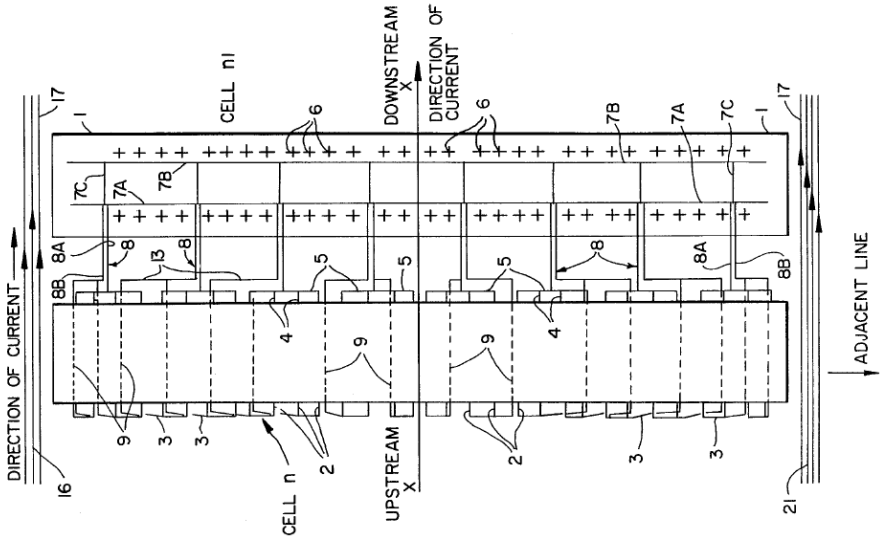

Figure 4. Busbar design presented in Figure 3 of [5].

Figure 3 of [5] shows the impact of the two extra, independent compensation busbars (16 and 21 in Figure 4). They significantly reduce the B_z longitudinal gradient. For the example of a 480 kA cell under the influence of a return potline located 65 meters away, 105 kA is passed in busbar 16, and 180 kA is passed in busbar 21 in order to produce symmetric B_z magnetic field within the range of ± 2.3 mT. It is also specified in this example that the two extra compensation busbars 16 and 21 are located 1.5 meters away from the potshell end walls.

Figure 5 shows the model setup of a 500 kA cell using the second busbar concept developed by the author and presented in Figure 2 of [4]. Figure 6 shows the B_z field obtained, which is also shown in Figure 2 of [4]. The B_z magnetic field is fairly symmetric and within the range of ± 1.7 mT.

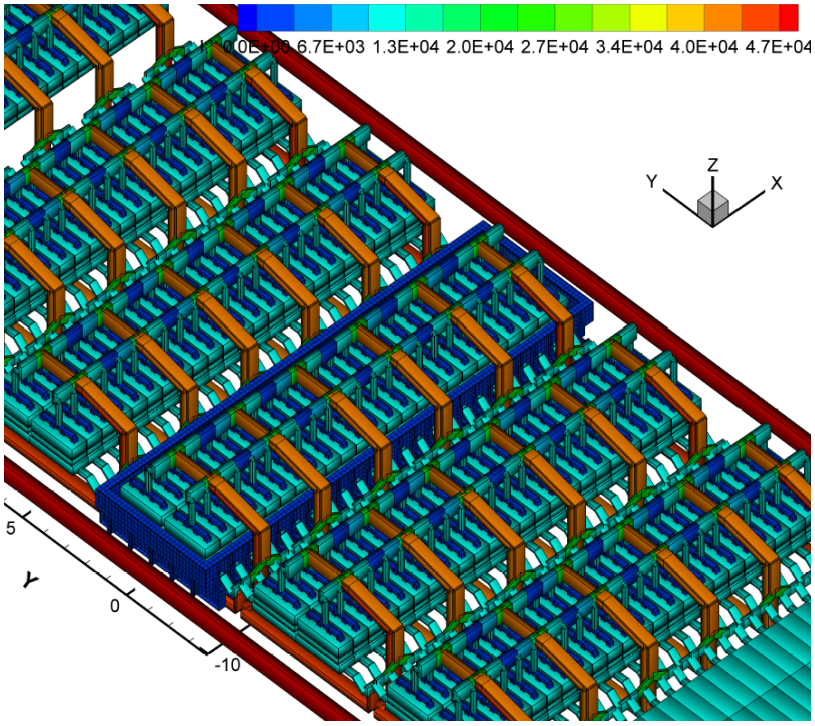

Figure 5. Busbar design of a 500 kA cell presented in Figure 2 of [4].

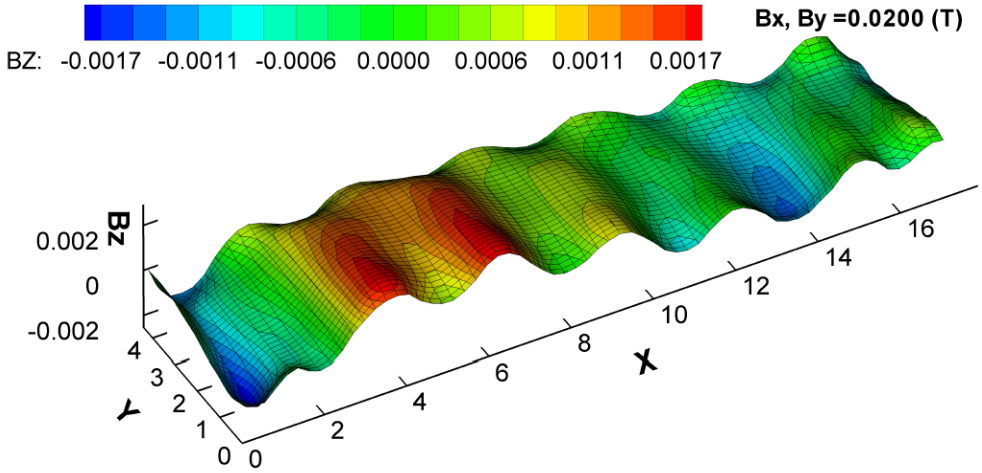

Figure 6. B_z of the busbar design in Figure 5 also presented in Figure 2 of [4].

The third busbar network concept was patented by Hydro Aluminium in 2006 [6]. It is simply a mix of the above two busbar concepts. According to the Hydro Aluminium patent, there is an optimal mix of the first concept, designated as ICC (Internal Compensation Current) and the second concept, designated as ECC (External Compensation Current). The ICC leads to a quadratic increase of the busbar weight when cell amperage is increasing, while the ECC is characterized by a linear increase of the busbar weight when cell amperage is increasing. Yet, the ECC starts with a bigger weight than the ICC. Up to 500 to 600 kA, it may be that ICC remains more advantageous to use than ECC.

The new busbar network concept designated CCC (Combined Compensation Current) is the optimal mix of ICC and ECC. It starts to be advantageous to use in place of ICC at around 250 to 300 kA and similarly to ECC, is characterized by a linear increase of the busbar weight when the cell amperage is increasing. CCC is always more advantageous to use than ECC.

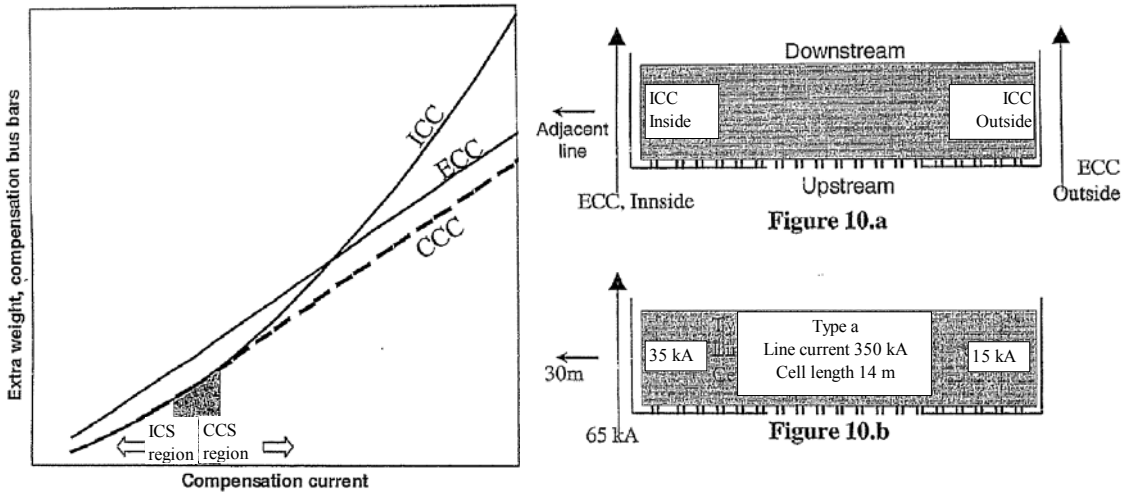

Figure 7: CCC busbar concept presented in Figures 6 and 10 of [6].

For the example of a 350 kA cell under the influence of a return potline located at only 30 meters away, 35 kA of ICC is passing around the cell on the left or on the inside, 15 kA is passing around the cell on the right or on the outside, leaving 125 kA passing directly under the cell. In addition, 65 kA of the ECC is passing to the left. There is no need for ECC on the right side in this example. Qatalum smelter's HAL 250 cell technology may be using CCC, since the return pot row is in the same building (Figure 8 – left) with small distance between rows, therefore strong magnetic compensation is needed. The right picture of Figure 8 is actually showing two potlines, not only one.

Figure 8. Qatalum smelter potroom with two rows of HAL 250 cells (left) [7] and the smelter with two potlines (right) [8].

3. New, fourth busbar concept: RCC (Reversed Compensation Current)

RCC is a completely different busbar network concept when compared to the previous three types, ICC, ECC and CCC, but the purpose is the same: to minimize the B_z, and provide a scalable solution to the cell stability problem for any cell amperage.

RCC is similar to ECC in two ways: there is no ICC, so there is no internal current busbars going around the cells, and the B_z generated by the busbars passing directly under the cell is compensated by external current busbars. But contrary to ECC, these extra compensation busbars:

1) Are passing under the cell close to the internal current busbars passing under the same cell

2) Are carrying current traveling in the opposite direction as the potline current.

There are two major versions of RCC. In the initial version, this is the only innovation. In the second most recent version, there is a second innovation: downstream risers, which are risers located on the downstream side of the cell, feeding the downstream anode beam.

3.1. First version of RCC

The first version of the RCC does not involve using downstream risers. In the simplest version of RCC, 100 % of the potline current is returned in extra compensation busbars running under the cells. This is a perfectly valid and scalable way to minimize the B_z. Results of the first version of RCC have been first presented in [9] in 2006 for cells running at 500 and 740 kA.

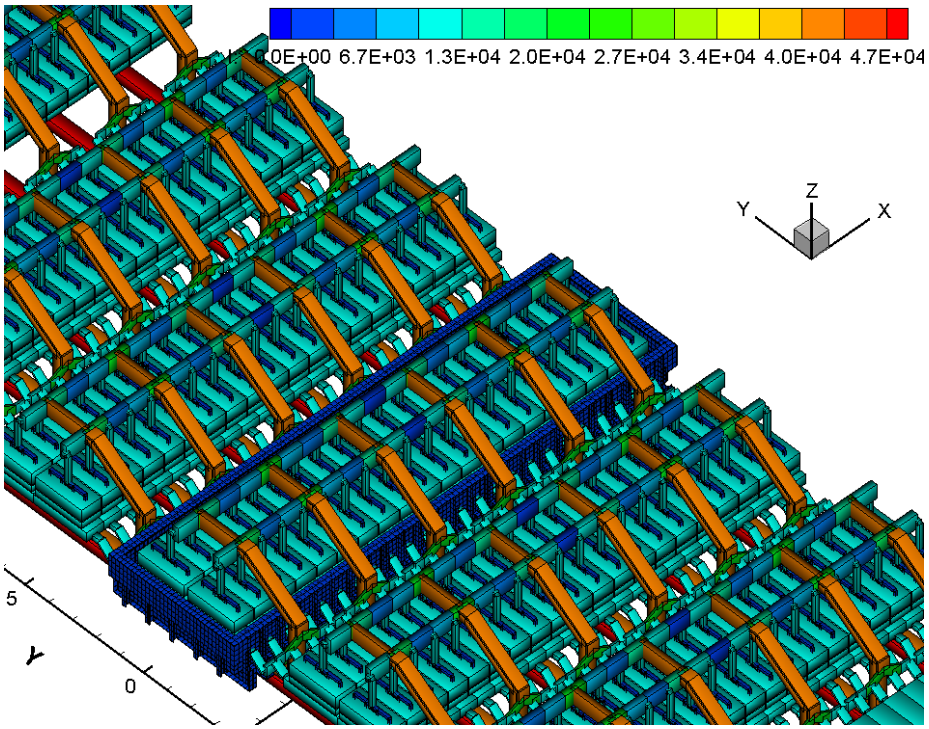

Figure 9. RCC busbar design of a 500 kA cell.

The model setup of the first RCC busbar design is presented for the first time in Figure 9, yet B_z, the vertical magnetic field component, obtained and presented in Figure 10 was presented in Figure 5 of [9] in 2006 for the first time. The B_z magnetic field is fairly symmetric within the range of ± 1.8 mT. There are six upstream side busbars passing under the cell feeding current to the six risers. In tandem, there are six extra compensation busbars passing directly under these six underside busbars. Together, these six extra compensation busbars are carrying the full line current, but in the opposite direction.

In 2006, the impact of this RCC busbar design on the B_x, and subsequently on the steady state bath/metal interface deformation, was overlooked. It turns out that the first version of RCC accentuates the B_x offset towards almost 100 % negative values, as can be seen in Figure 11, produced later using a different version of the code MHD-VALDIS. This B_x in turn produces almost 100 % positive transverse electromagnetic force component, F_y, which finally produces the steady-state bath/metal interface that is also presented in Figure 11. The metal level is about 14 cm higher on the downstream side in comparison to the upstream side. This asymmetry of the steady-state bath/metal interface deformation is not unique in this first version of RCC, but is more accentuated than in the other busbar configurations. This may or may not constitute a problem.

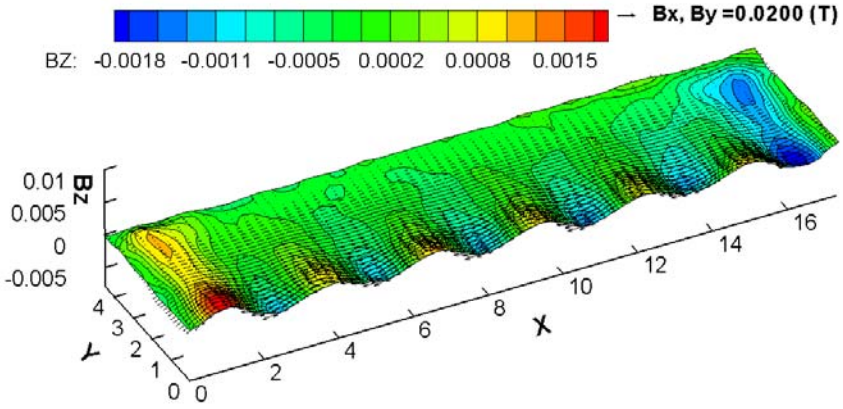

Figure 10. B_z from the busbar design in Figure 9, already presented in Figure 5 of [9].

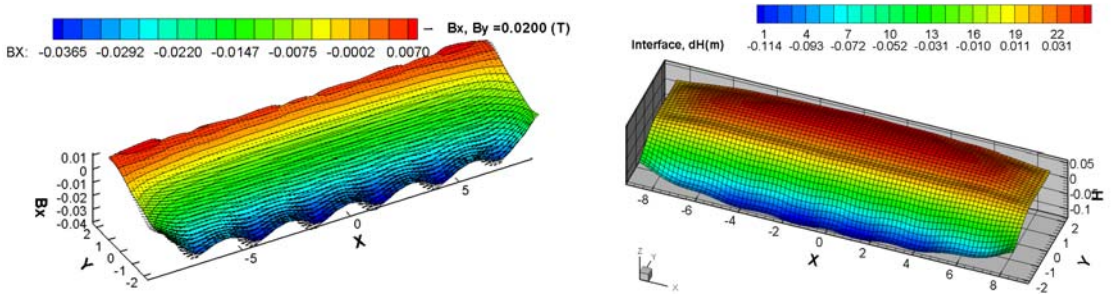

Figure 11. B_x and steady-state bath/metal interface from the busbar design in Figure 9.

Nevertheless, this first version of RCC is a perfectly scalable way to minimize the B_z as demonstrated with the 740 kA cell case presented in [9] in 2006 and shown in Figure 12, right. The busbar design for this cell is shown in Figure 12, left. This 740 kA cell is 50 % longer than the 500 kA cell, and has nine risers instead of six. There are nine compensation busbars in tandem with the nine upstream side busbars passing under the cell carrying the full line current in the opposite direction.

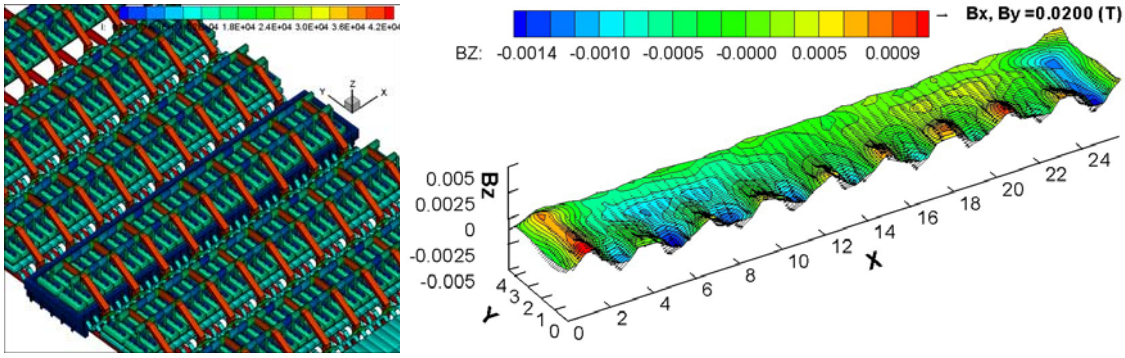

Figure 12. RCC busbar design of a 740 kA cell and resulting B_z.

3.2. Second version of RCC

For this second version of RCC, a new design criterion was added. The design must produce a perfectly anti-symmetric B_x in addition to minimizing the B_z, all the while remaining perfectly scalable. In order to do so, downstream risers are required. In this second RCC version, all the potline current is passing in internal busbars under the cells. Upstream side busbars carry half of the potline current from the upstream side of the cell to the upstream risers of the next cell passing under the cell. Downstream side busbars also carry half of the potline current from the

downstream side of the cell to the downstream risers of the next cell passing under the next cell. As in the first RCC version, in tandem, extra compensation busbars are carrying the full line current in the opposite direction. Figure 13 presents the busbar layout for the 740 kA cell with 18 risers and the 1500 kA cell with 36 risers.

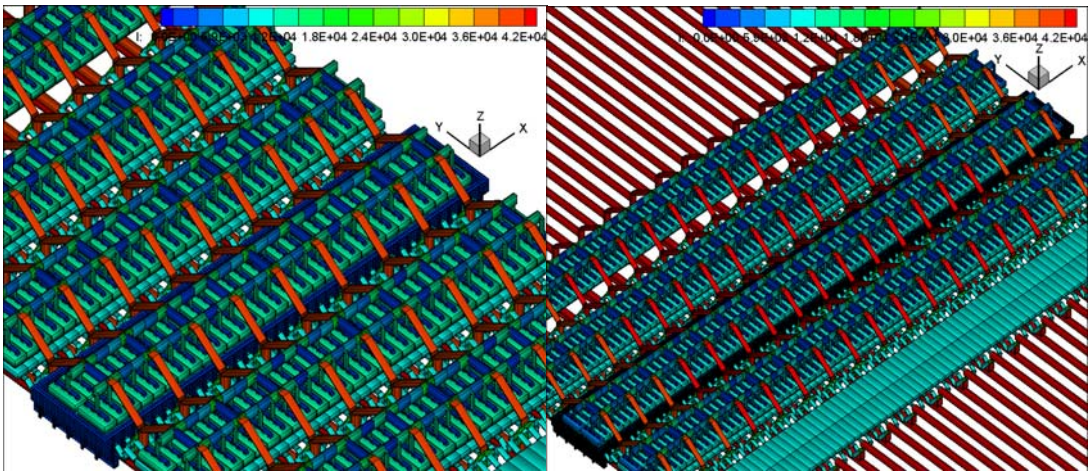

Figure 13. RCC busbar design of a 740 kA cell and a 1500 kA cell.

The resulting B_z, B_x, bath/metal steady-state deformation and steady-state metal flow are presented in Figure 14 for the 740 kA cell, and in Figure 15 for the 1500 kA cell. Notice that the B_x is now almost perfectly anti-symmetric and as a result, the bath/metal deformation is perfectly symmetric. For the 1500 kA cell case, some of these results have been already presented in [10]. These results demonstrate that the RCC busbar concept is perfectly scalable to any cell size. MHD-VALDIS transient analysis was also carried out, predicting that both cells will be extremely stable. Results of the cell transient stability analysis for the 1500 kA cell are presented in Figure 9 of [10]. Since the usage of downstream risers will increase the busbar weight, the next phase would be to test both versions of RCC to see if downstream risers are absolutely required or not.

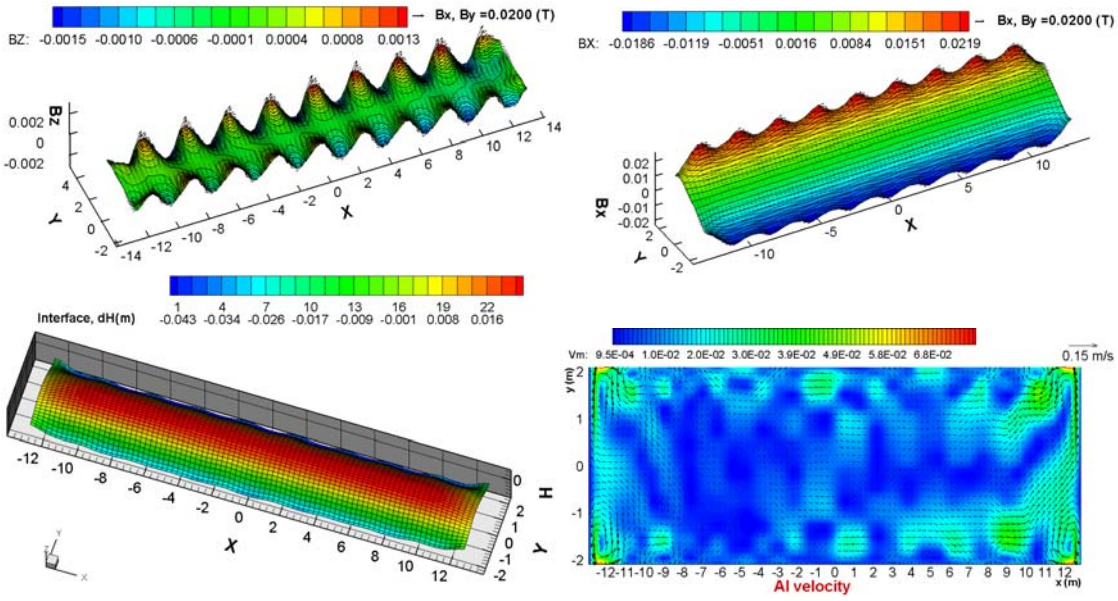

Figure 14. B_z, B_x, bath-metal interface deformation and metal flow in second version RRC busbar design for the 740 kA cell.

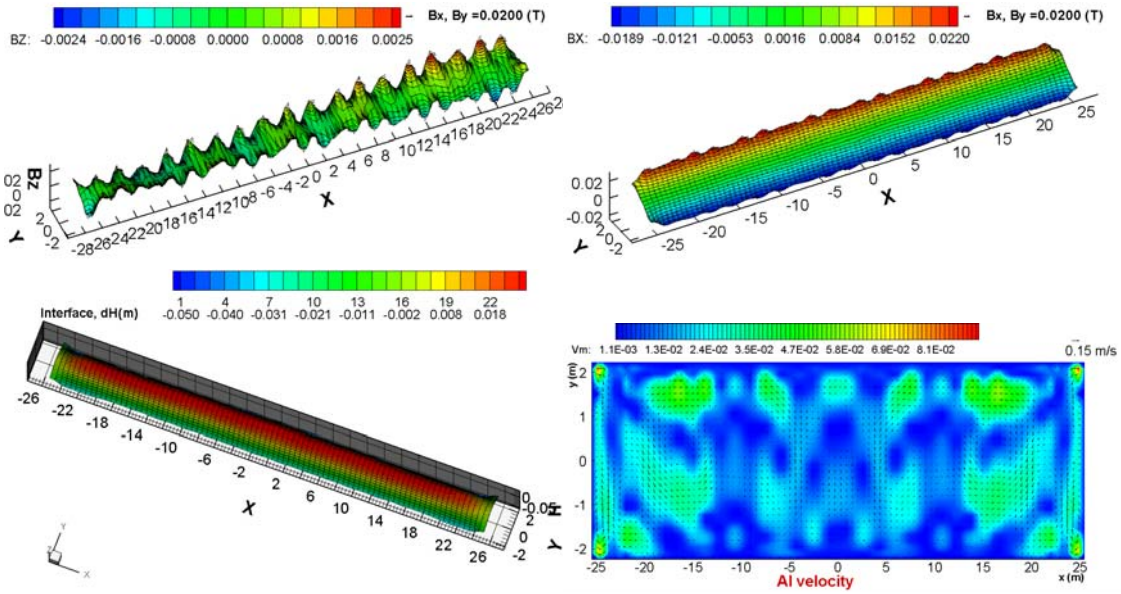

Figure 15. B_z, B_x, bath-metal interface deformation and metal flow in second version RRC busbar design for the 1500 kA cell.

4. RCC usage opportunities for future smelter design

The main concept of RCC is to carry the full potline current in the "extra" compensation busbars under the cells in the opposite direction. This creates the option to return the potline current in these compensation busbars instead of in a return pot row located in a second potroom. Therefore, the option to design smelters with an odd number of potrooms becomes available. The fact that the compensation busbars carry the same current as the potline in the opposite direction also means that there is no net current running in the potline, meaning that that potline will have absolutely no magnetic influence on a neighboring potline. Therefore, potlines can be placed very close to each other in the same building if desired. Figure 16 illustrates the case of a smelter having three independent potlines in a very compact footprint. Alternatively, a smelter could be made of a single very long potline/potroom.

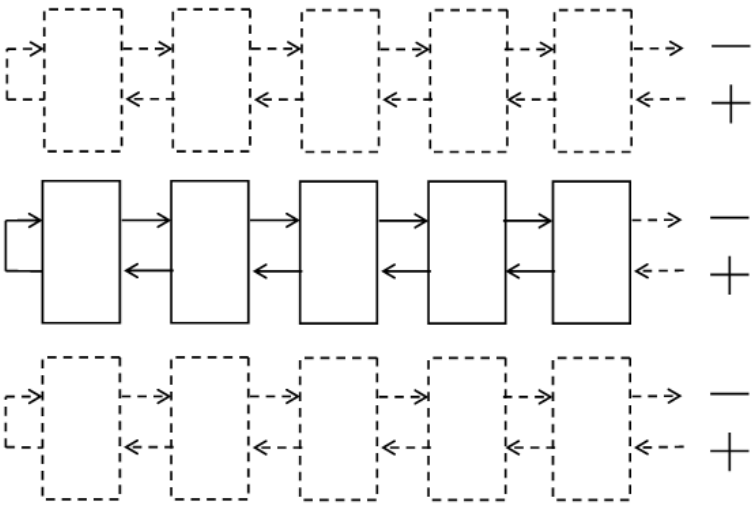

Figure 16: Smelter having three independent potlines in a very compact footprint.

5. Conclusions

A completely new busbar network concept has been developed called RCC - reversed compensation current. RCC has the advantage of being easily extendable to any electrolysis cell size. RCC is similar to ECC for two reasons: there is no ICC, so no internal current busbars passes around the cells, and the B_z generated by the busbars passing directly under the cell is compensated by external current busbars. But contrary to ECC, these extra compensation busbars:

1) Are passing under the cell close to the internal current busbars already passing under the same cell.
2) Are carrying current traveling in the opposite direction as the potline current.

There are two major innovations in two different versions of RCC. In the initial version, the first and most important innovation is that the external compensation current is passing under the internal current busbars passing under the cell but in the opposite direction. In the second most recent version, there is a second innovation: downstream risers located on the downstream side of the cell. The usage of downstream risers ensures that the B_x is anti-symmetric so the bath/metal interface deformation is symmetric.

Results have been presented for cells operating at 500, 740, and 1500 kA, clearly demonstrating that the RCC busbar network concept is perfectly scalable to any cell size and amperage. RCC opens the door to the possibility to design smelters with an odd number of potrooms, and to locate multiple potrooms in a very compact footprint.

6. References

1. N. Urata, Wave Mode Coupling and Instability in the Internal Wave in the Aluminum Reduction Cells, TMS Light Metals 2005, pp 455-460.
2. P. Davidson, A Introduction to Magnetohydrodynamics, Campridge Texts in Applied Mathematics, Cambridge University Press 2001, pp. 363-386.
3. Ding Ji-lin, Li Jie, Zhang Hong-liang, Xu Yu-jie, Yang Shuai and Liu Ye-xiang, Comparison of structure and physical fields in 400 kA aluminum reduction cells, J. Cent. South Univ. (2014) 21, pp 4097−4103.
4. M. Dupuis and V. Bojarevics, Retrofit of a 500 kA cell design into a 600 kA cell design, ALUMINIUM 87(1/2) (2011), pp 52-55.
5. Joseph Chaffy, Bernard Langon and Michel Leroy, Device for connection between very high intensity electrolysis cells for the production of aluminium comprising a supply circuit and an independent circuit for correcting the magnetic field, US patent no 4713161 (1987).
6. Glenn Ove Linnerud and Reidar Huglen, Method for electrical connection and magnetic compensation of aluminium reduction cells, and a system for same, WO patent no 2006/033578 and US patent no 8070921 (2011).
7. Innovations in Pot Tending at the Qatalum Smelter, Qatar Aluminium Google+ post, (Nov 2014). https://plus.google.com/photos/+QatarAluminiumqatalum/albums/6083295683970456401
8. Jørgen C. Arentz Rostrup, Hydro – a leading integrated aluminium and energy company, BMO Global Metals & Mining Conference, (2010). http://www.hydro.com/upload/Documents/Presentations/Other/2010/010310%20-%20BMO%20-%20JR.pdf .
9. M. Dupuis and V. Bojarevics, MHD and pot mechanical design of a 740 kA cell, ALUMINIUM 82(5) (2006), pp 442-446.
10. M. Dupuis and V. Bojarevics, Newest MHD-Valdis cell stability studies, ALUMINIUM 90(1/2) (2014), pp 42-44.